Cranfield

College of Aeronautics Report No.9017
July 1990

CRANFIELD INSTITUTE OF TECHNOLOGY
LIBRARY

REVIEW OF INITIAL EXPERIMENTS USING THE HAWK MODEL, DYNAMIC RIG FACILITY AND THE CED1401 DIGITAL DATA ACQUISITION EQUIPMENT

H.A.Hinds and M.V.Cook

Seventh Quarterly Report
July 1990

College of Aeronautics
Cranfield Institute of Technology
Cranfield, Bedford MK43 0AL. England

1401288156

Cranfield

College of Aeronautics Report No.9017
July 1990

CRANFIELD INSTITUTE OF TECHNOLOGY LIBRARY

REVIEW OF INITIAL EXPERIMENTS USING THE HAWK MODEL, DYNAMIC RIG FACILITY AND THE CED1401 DIGITAL DATA ACQUISITION EQUIPMENT

H.A.Hinds and M.V.Cook

Seventh Quarterly Report
July 1990

College of Aeronautics
Cranfield Institute of Technology
Cranfield, Bedford MK43 0AL. England

ISBN 1 871564417

£10.00

"The views expressed herein are those of the authors alone and do not necessarily represent those of the Institute"

COLLEGE OF AERONAUTICS REPORT
9017

REVIEW OF INITIAL EXPERIMENTS USING THE HAWK MODEL, DYNAMIC RIG FACILITY AND THE CED1401 DIGITAL DATA ACQUISITION EQUIPMENT.

Prepared by H.A.Hinds and M.V.Cook

SEVENTH QUARTERLY REPORT

JULY 1990

College of Aeronautics
Cranfield Institute of Technology
Cranfield
Bedford MK43 OAL

ACKNOWLEDGEMENTS

The research which is the subject of this report was initiated by MOD(PE), Aerodynamics Dept., Royal Aerospace Establishment, Farnborough, in response to a proposal by the College of Aeronautics under the terms of Agreement No.2082/192.

The support and encouragement of the technical monitor, Dr. A.J. Ross is gratefully acknowledged.

"The views expressed herein are those of the authors alone and do not necessarily represent those of the Institute"

CONTENTS PAGE

1.0	INTRODUCTION	3
2.0	CALIBRATION OF CONTROL SURFACE ANGLES	5
3.0	DATA ACQUISITION SYSTEM	9
	3.1 Recording of data	9
	3.2 Removal of noise	9
	3.3 Disadvantage of the CED1401	10
	3.4 Conversion of CED1401 data	11
4.0	MEASUREMENT OF MOMENTS OF INERTIA	12
	4.1 Pitch	12
	4.2 Yaw	16
	4.3 Roll	19
5.0	MSR PROGRAM	20
6.0	CONCLUSION	21
	REFERENCES	22
APPENDIX A:	GRAPHICAL ANALYSIS OF DATA	23
APPENDIX B:	ESTIMATION OF NON-DIMENSIONAL DERIVATIVES	26

1.0 INTRODUCTION.

This report is concerned with work carried out during the last quarter which is part of an on-going programme of research to evaluate the use of a modified stepwise regression (MSR) procedure to predict aircraft stability and control derivatives (REF 1). The main objective of the last quarter has been to test the Hawk model, the dynamic wind tunnel facility, the data acquisition system and to check that everything is in a good working order.

Following recent investigations of the longitudinal static stability of the Hawk model, (REF 2), the model support gimbal has been moved forward 10mm. This was done to improve the stick-fixed static stability margin of the model and to make it easier to control and trim in the wind tunnel. This has been confirmed in practice. After initial experimentation with the model restrained in height when flown in the wind tunnel, a couple of inches of freedom in vertical height was allowed. It was found that the model did not take off as "violently" as in the past with the old gimbal position.

When the elevator control angle is reduced to get the aircraft to lift off there is still a noticeable friction between the model gimbal and vertical rod to be overcome. Once flying, the elevator may be increased slightly to trim the Hawk without the model stalling, thus indicating the presence of the initial friction. This has been improved by lubrication of the vertical rod and gimbal.

Another problem associated with a change of vertical height of the model is that the tunnel speed also changes slightly due to various blockage effects. It is recommended that the tunnel speed should be allowed a few minutes to settle down after "take-off" and trimming of the model before any data is recorded.

Laterally, the model is very sensitive to small disturbances in the wind tunnel airflow and is therefore very difficult to trim in roll. This problem is not helped by the fact that the Weybridge wind tunnel is an open jet facility with a diameter of 1.06m and the Hawk model wing span is 0.78m. However, the use of an attitude angle (or attitude rate) feedback control loop is very successful in helping to trim the model in roll.

It is found that the model is best trimmed if the roll angle (ϕ), multiplied by a gain of around k = 0.15, is fed back to the aileron input. If a feedback gain of more than about 0.2 is used the control input to the aileron overcompensates for the roll angle and the model can be made to "wing rock" quite nicely!

Roll attitude feedback is normally de-stabilising and therefore not often used, but in the case of the dynamic facility it is simple to apply and with low gains it serves a useful purpose in helping to compensate for disturbances in the tunnel flow. It is realised that roll attitude rate feedback would be much better than roll attitude angle feedback. However, there are several practical problems with the generation of data for a roll rate feedback loop, although it is not impossible to do so.

In yaw, the model appears to be very stable although it is difficult to read small changes in the angle of yaw (or side slip as experimentally $\beta = -\psi$) due to backlash in the yaw position sensing system. The wiper of the yaw potentiometer has been glued into the vertical rod to try to prevent the wiper falling out and not moving with the vertical rod which rotates with the model. This made it difficult to hold the main body of the potentiometer in a fixed position relative to the wiper and previous attempts to measure the yaw inertia I_z of the model were impossible because of this problem (REF 2). A foam packaging has now been placed around the yaw pot to hold it in place. This has improved the situation for large angles of yaw but not for the smaller angles.

2.0 CALIBRATION OF CONTROL SURFACE ANGLES.

The control surfaces of the Hawk model are driven by three electrical servo actuators mounted inside the model fuselage. The servos are very sensitive to the polarity of the input voltage, as discovered when the aileron, elevator and rudder servos were connected the wrong way round. A reversal of the voltage caused damage to the internal circuitry of the servos. Two spare servos were used for the aileron and elevator control surfaces whilst repairs were made to the rudder servo. The rudder on the model was held in place using tape and it was still possible to fly the model in the tunnel.

When the rudder servo was replaced, it was noted that a rudder control surface angle of ρ = 0 on the model corresponded to an input voltage of ~-0.504V (from the 0V direction). This is due to the "zero" position of the servo with no power which would need to be changed to provide a more suitable scale for the rudder control surface voltage. However, this is not easily achieved and it is thought that the present position is acceptable as a control surface input range of $\pm 15^{\circ}$ should prove to be more than adequate.

To calibrate the aileron, elevator and rudder control surfaces the model was placed on a level bench with the wing leading and trailing edges in a straight and level reference attitude. A pointer was attached to the port aileron and the control surface angles set in various positions with respect to a marked scale on some polar graph paper. For each aileron angle the input and output voltages of the servo were recorded. Due to backlash in the control system it is necessary to record two sets of input and output voltage data for the control surface, going from a +ve to -ve angle and vice-versa.

A similar procedure was carried out for the elevator and rudder control surfaces. Calibration graphs for all three control surfaces are show on the following pages. The calibrations of the model attitude angles are due next.

ELEVATOR CONTROL SURFACE CALIBRATIONS.

ELEVATOR CALIBRATIONS (T.E. UP TO DOWN)

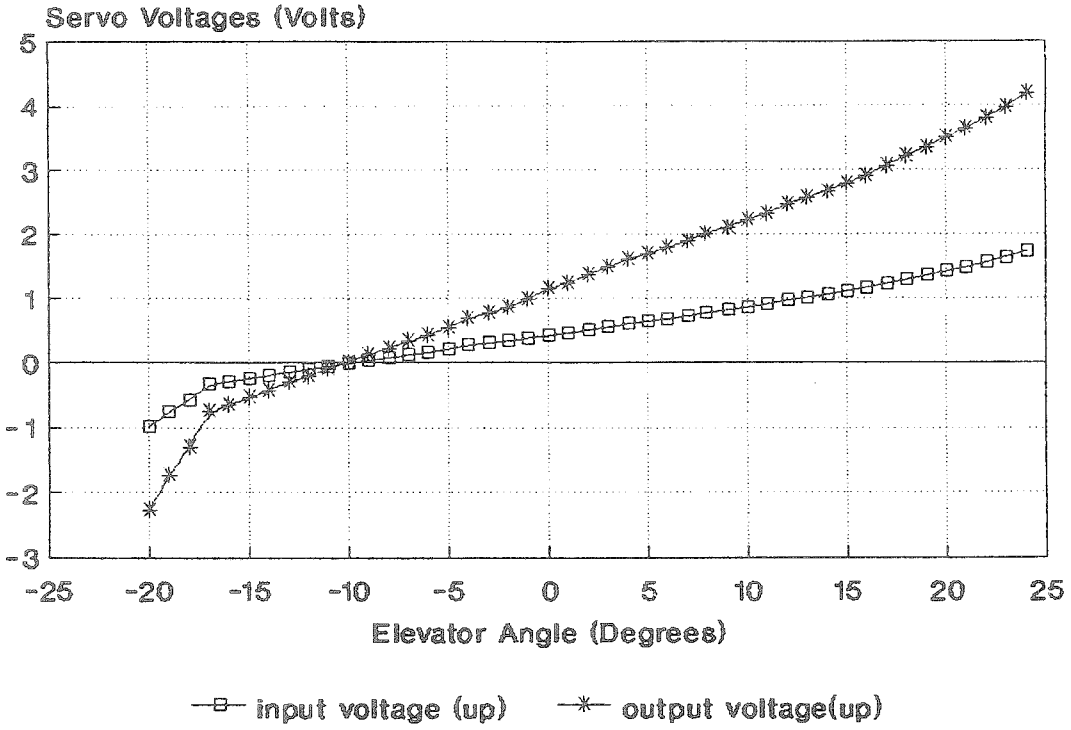

ELEVATOR CALIBRATIONS (T.E. DOWN TO UP)

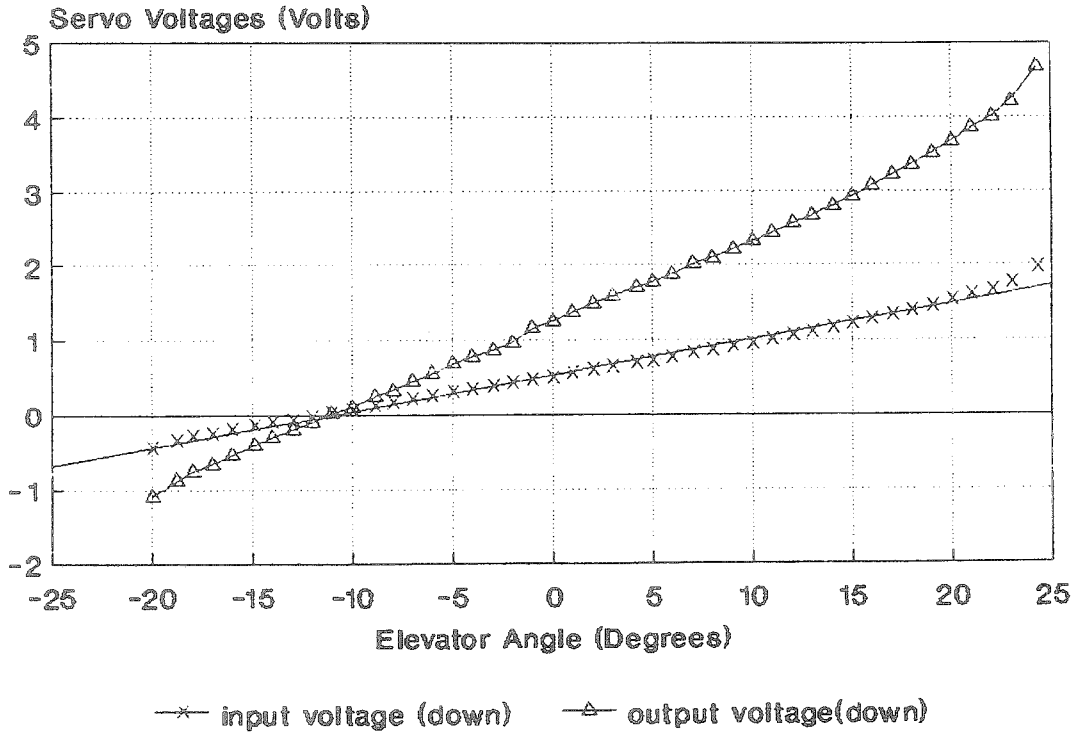

AILERON CONTROL SURFACE CALIBRATIONS.

AILERON CALIBRATIONS (T.E. UP TO DOWN)

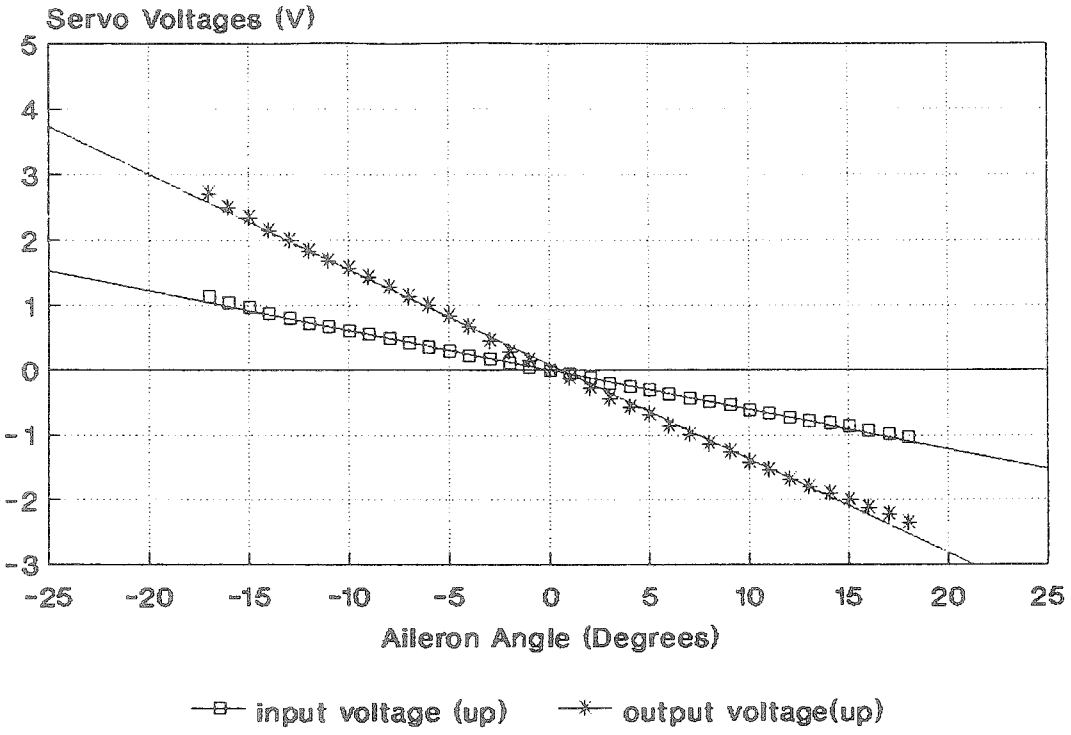

AILERON CALIBRATIONS (T.E. DOWN TO UP)

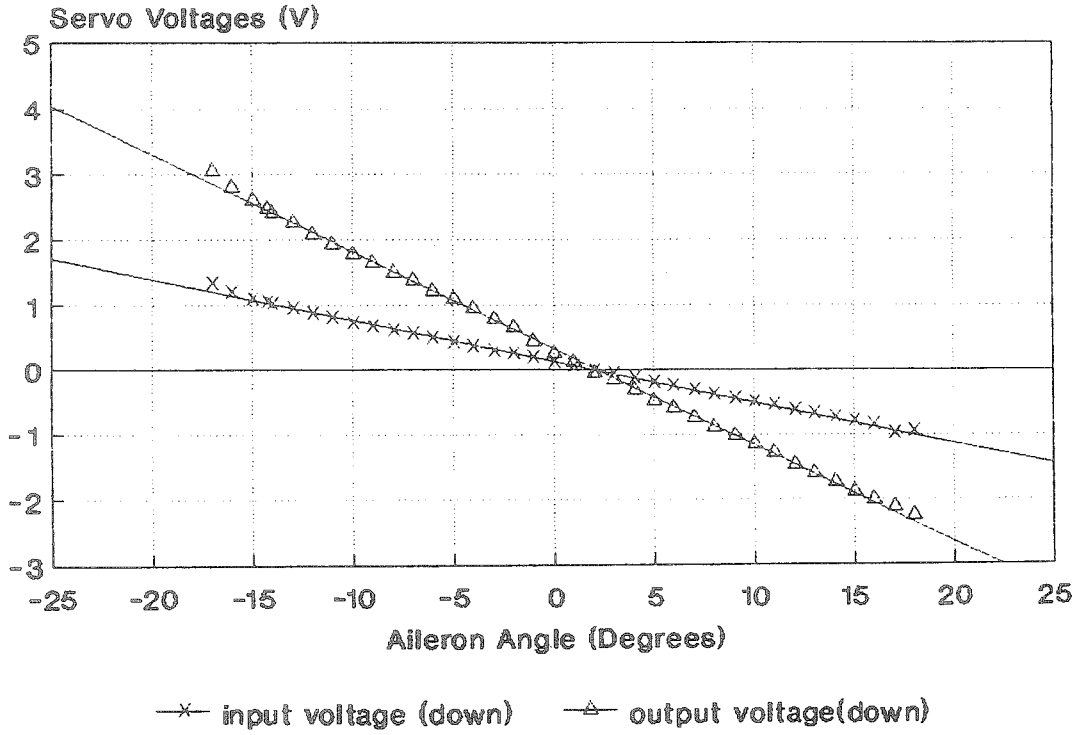

RUDDER CONTROL SURFACE CALIBRATIONS.

RUDDER CALIBRATIONS (PORT TO STARBOARD)

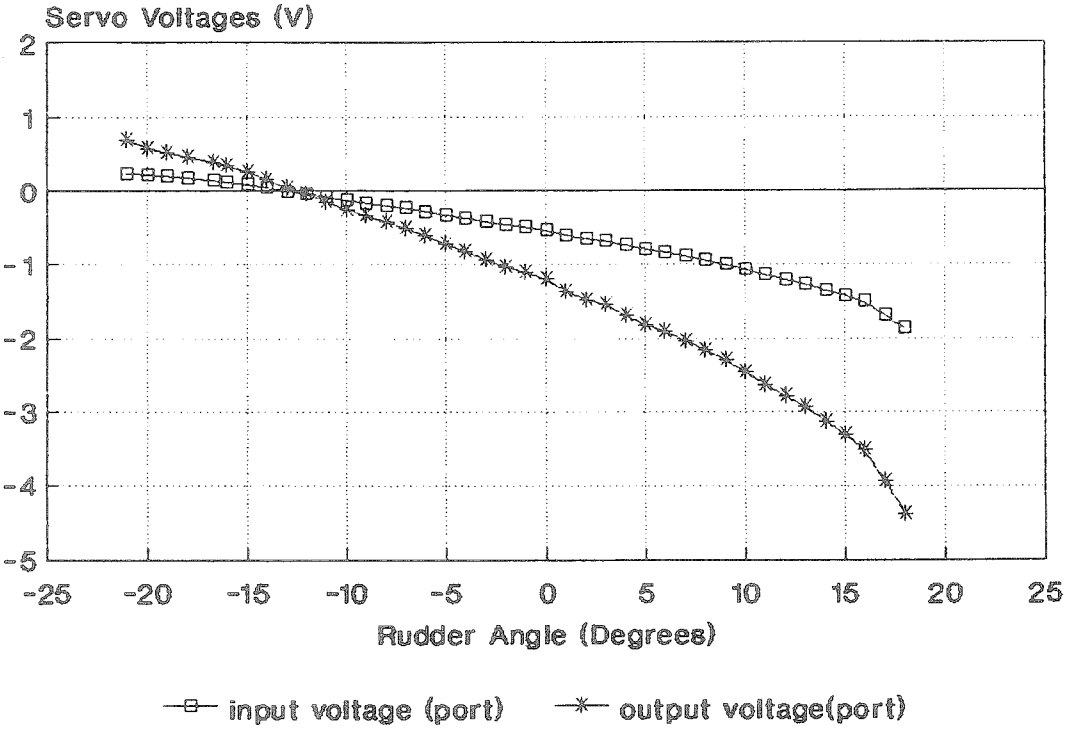

RUDDER CALIBRATIONS (STARBOARD TO PORT)

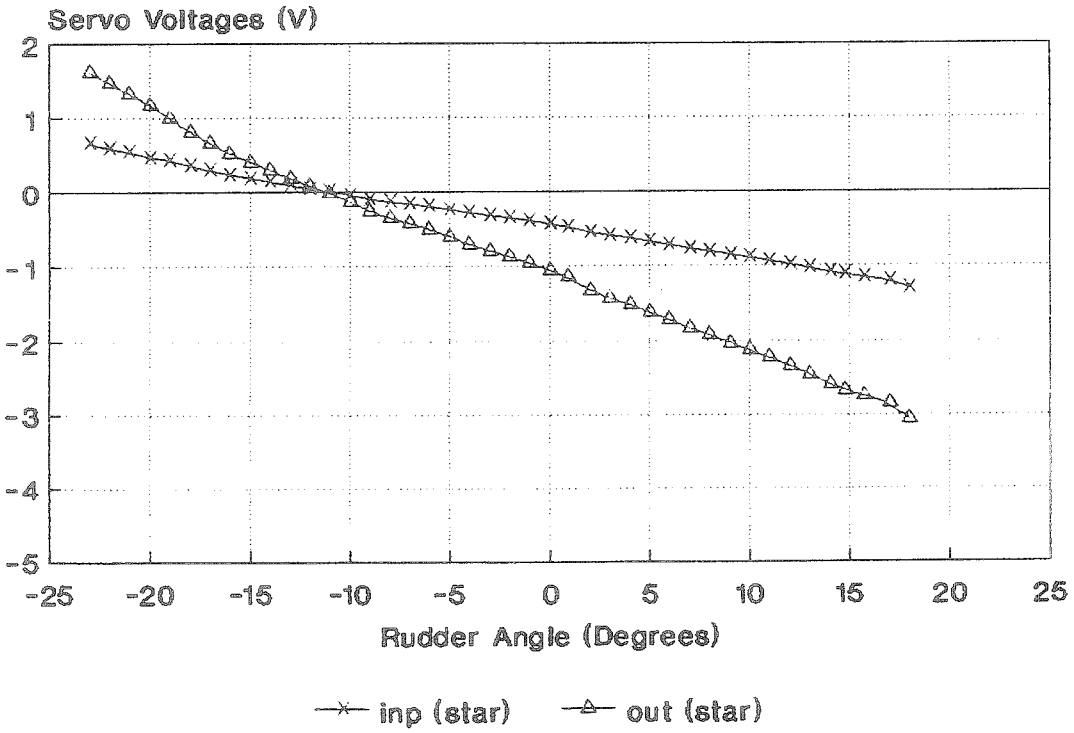

3.0 DATA ACQUISITION SYSTEM.

The data acquisition system was initially tested using the Waterfall software on the IBM computer. This software enables the experimenter to monitor and check incoming signals to the CED1401 before any signals are actually recorded. It was found that the signals from the electronic control unit (ECU) were extremely noisy and when all the inputs on the ECU were grounded with 0V the noise was even worse. Eventually, it was discovered that there were only 8 connections from the ECU to the CED1401 corresponding to the input channels C8 to C15. As there was no common ground of 0V between the two pieces of equipment there was a lot of noise. When a connection was made from a 0V output on the ECU to an input for ground on the CED1401 the magnitude of the noise decreased dramatically.

3.1 Recording Of Data.

A TURBO-PASCAL program called REC8.PAS has been written to record data simultaneously from channels C8 to C15 with no time delay between the sampling of each channel. This program was used extensively to record various wind-on and wind-off oscillations in pitch, yaw and roll for the calculation of various inertias and aerodynamic damping derivatives, as described in section 4.0. A number of different sampling rates have been used as it is very easy to change the REC8.PAS program as required.

3.2 Removal Of High Frequency Noise.

A sampling frequency of 100 Hz was used in the inertia experiments as this speed was found to provide an adequate number of data points for one period of oscillation of the Hawk model. There was still a great deal of noise associated with the data. In order to remove this noise two programs have been written in TURBO-PASCAL and called FILT.PAS and MEANFILT.PAS.

Both of these programs use CED spectrum array arithmetic routines to filter out high frequency noise from the recorded data files, (REF 3). The FILTER routine uses a low.pass Butterworth digital filter. Details of the characteristics of this filter are well known and may be found in many text books, such as Horowitz and Hill (REF 4). To cancel out any change in phase the filter is used twice to pass the data through in one direction and then the other. This was checked by examining files before and after filtering and confirming that the peaks and troughs of the data were in the same place (ie at the same times) and the magnitudes had not been affected.

The MEANFILT.PAS program used another routine to find the mean value of a set of data points called AVERAGE. A second routine (called SHIFT) is then used to remove the mean/DC component of the data. The data is then filtered twice using FILTER. This program was useful as the inertia oscillations were never around 0V and it is easy to shift the position of the oscillations using MEANFILT.PAS. This made it a lot easier to expand the voltage scale showing the oscillations using waterfall to read the voltages and times of peak and minimum voltages.

3.3 Disadvantage Of The CED1401.

If any signal to the CED1401 is greater than ±5 Volts a flat voltage of ±5 Volts is recorded. This means that signals exceeding this limit will have to be scaled down using potentiometers introducing further noise (and possible time delays).

3.4 Conversion Of CED1401 Data.

The CED1401 stores data as integers between -32768 and +32767 as a signed 16 bit number (stored low byte first and then high byte). A program has been written in TURBO-BASIC called CONVERT.BAS to read these date files, convert the pairs of bytes to an integer and then further convert this integer to a voltage using volts = (integer/32767)*5 for 0 < integer ≤ 32767 or volts = [(integer - 65536)/32767]*5 for integer > 32767. (Note that an integer > 32767 AND ≤ 65535 implies a -ve voltage). This basic program then outputs the data as a voltage to 3 d.p.

A second program called CONDIF.BAS will convert any data files to volts and also provide the first and second differentials of the signal y if required using the following formulae, where h is the time step between successive points:

$$y'_i = (-y_{i+2} + 8y_{i+1} - 8y_{i-1} + y_{i-2}) / 12h \qquad \text{EQN(1)}$$

$$y''_i = (-y_{i+2} + 16y_{i+1} - 30y_i + 16y_{i-1} + y_{i-2}) / 12h^2 \qquad \text{EQN(2)}$$

It should be noted that for both y'_i and y''_i the first two and last two data points in a file are lost as they are needed to obtain the differentials of y at point y_i.

Both of the basic programs have been written so that they can read in more than one channel of data to form a data file of the format required as input to the MSR FORTRAN 77 program.

For example is C8 recorded η, C9 recorded θ, the two channels could be combined to form a file with the columns:

$\eta(t)$ $\theta(t)$ $q(t)$ $\dot{q}(t)$

which would correspond to the MSR format of

$x_1(t)$ $x_2(t)$ $x_3(t)$ $y(t)$

4.0 MEASUREMENT OF MOMENTS OF INERTIA.

The pitch, yaw and roll moments of inertia and the pitch and yaw aerodynamic damping derivatives have been found using the free oscillation method described in the previous report (REF 2). All of the data files for the wind-on and wind-off experiments were obtained using the CED1401 data acquisition system. All the peaks, troughs and associated times and periods were estimated from data files which had been filtered to remove high frequency noise and centre the oscillation about 0 volts. Appendix A presents further details of the graphical analysis of the recorded oscillations.

4.1 PITCH

The reduced model equation of motion may be expressed as follows (REF 5):

$$\mathring{Z}(t) = -\mathring{M}_w.w - \mathring{M}_{\dot{w}}.\dot{w} - \mathring{M}_q.q + I_y.\dot{q} \qquad \text{EQN(3)}$$

Noting that $q = \dot{\theta}$; $\dot{q} = \ddot{\theta}$; $w = U\infty.\theta$; $\dot{w} = U\infty.\dot{\theta}$; and adding in the frictional term $-f_y.\theta$ and spring stiffness term $K.\theta$, leads to the following equation:

$$I_y.\ddot{\theta} + (-\mathring{M}_q - \mathring{M}_{\dot{w}}.U\infty - f_y).\dot{\theta} + (-\mathring{M}_w.U\infty + K).\theta = 0 \qquad \text{EQN(4)}$$

where $K = l^2.(k4 + k5)$

l = distance from c.g. to wire attachment point = 0.46m

$k4+k5$ = sum of spring constants = 63.5 N/m

Equation (4) may also be expressed in the form:

$$\frac{d^2\theta}{dt^2} + 2\zeta\omega_o.\frac{d\theta}{dt} + \omega_o^2.\theta = 0 \qquad \text{EQN(5)}$$

where: ζ = system damping ratio.

ω_o = system undamped natural frequency.

OR in the form:

$$\frac{d^2\theta}{dt^2} + a.\frac{d\theta}{dt} + b.\theta = 0 \qquad \text{EQN(6)}$$

Comparing equations (4), (5) and (6) and noting a particular solution of equation (5) giving the amplitudes of the peaks and troughs to be $\theta = \theta_o e^{-\mu t}$, where $\mu = -\zeta\omega_o$, leads to the following identities:

$$a = 2\zeta\omega_{o_n} = -2\mu_{o_n} = (-\mathring{M}_q - \mathring{M}_w.U_\infty - f_y)/I_y \qquad \text{EQN(7)}$$

$$\text{and} \quad b = \omega_{o_n}^2 = (-\mathring{M}_w.U_\infty + K)/I_y \qquad \text{EQN(8)}$$

WIND-OFF:

If the model is tested with the wind-off, the aerodynamic term $\mathring{M}_q$ of equation (7) is assumed to so small that it may be neglected. Further, U_∞ will be zero and the following terms may be defined for the wind-off case:

$$\omega_{o_{off}}^2 = K/I_y \quad \Rightarrow I_y = [l^2(k_1 + k_2)]/\omega_{o_{off}}^2 \qquad \text{EQN(9)}$$

$$2\mu_{o_{off}} = f_y/I_y \quad \Rightarrow f_y = 2.I_y.\mu_{o_{off}} \qquad \text{EQN(10)}$$

Experimental Wind-off Data: (from file P6A.C8)

T_{off} = 0.55 (s) ω_n^2 = 130.507 (r/s)^2

μ_{off} = -0.069 (r/s) $\omega_{o_{off}}^2$ = 130.512 (r/s)^2

Substituting the above values into equations (9) and (10) gives:

I_y = 0.103 kgm^2 or 0.076 slug.ft^2 (cf 0.079 kgm^2 expected)

f_y = -0.014 kgm^{2}r/s

WIND-ON:

Using (7) and noting that $f_y/I_y = 2\mu_{off}$ it can be shown that:

$$-\mathring{M}_q - \mathring{M}_{\dot{w}}.U\infty = 2.I_y.(\mu_{off} - \mu_{on}) \qquad \text{EQN(11)}$$

Similarly, using (8) and noting that $K/I_y = \omega_{o_{off}}^2$ it may be shown that:

$$\mathring{M}_w = -(I_y/U\infty).(\omega_{o_{on}}^2 - \omega_{o_{off}}^2) \qquad \text{EQN(12)}$$

Experimental Wind-on Data: (from file P10OND.C8)

T_{on} = 0.49 (s) ω_n^2 = 164.425 (r/s)^2

μ_{on} = -2.359 (r/s) $\omega_{o_{on}}^2$ = 169.99 (r/s)^2

Substituting the appropriate wind-off and wind-on values into equations (11) and (12) leads to

$$\mathring{M}_w = -0.126 \text{ kg.m/s}$$

$$-\mathring{M}_q - \mathring{M}_{\dot{w}}.U\infty = 0.47174 \text{ kg.m}^2/\text{s}$$

The experimental data wind-on was recorded at a tunnel speed of 65.4 mm H_2O which corresponds to $U\infty$ = 32.125 m/s.

The model parameters S = 0.115 m^2 and $\bar{c}$ = 0.148 m yields the following to non-dimensionalise the derivatives:

$$M_w = \mathring{M}_w / (0.5).\rho.U\infty.S.\bar{c} = \mathring{M}_w / 0.3349$$

$$-M_q - M_{\dot{w}} = (-\mathring{M}_q - \mathring{M}_{\dot{w}}.U\infty) / (0.5).\rho.U\infty.S.\bar{c}^2 = (-\mathring{M}_q - \mathring{M}_{\dot{w}}.U\infty) / 0.0496$$

$$\Rightarrow M_w = -0.376 \quad \text{and} \quad \Rightarrow (-M_q - M_{\dot{w}}) = 9.51$$

Appendix B gives details of the theoretical values of these non-dimensional derivatives (estimated by Malik, REF 6) and those estimated from the longitudinal static stability experiments carried out on the Hawk model. The results are summarised below, along with the percentage relative error between these results and the values of derivatives obtained experimentally.

Table 1

	Experimental	Theoretical (%)	Estimated (%)
M_w	-0.376	-0.248 (51%)	-0.363 (3.6%)
M_q		-6.30	
$M_{\dot{w}}$		-2.73	
$-M_q - M_{\dot{w}}$	9.51	9.03 (5.3%)	

4.2 YAW

The reduced model equation of motion may be expressed as follows (REF 5):

$$\mathring{N}(t) = -\mathring{N}_v.v - \mathring{N}_p.p + I_z.\dot{r} - \mathring{N}_r.r \qquad \text{EQN(13)}$$

If the oscillations are assumed to be purely a yawing action of the model the rolling term ($\mathring{N}_p$) may be ignored. Therefore, noting that $r = \dot{\psi}$; $\dot{r} = \ddot{\psi}$; $v = -U\infty.\psi$; and adding in the spring stiffness and frictional terms, $K\psi$ and $f_z\psi$ respectively, leads to:

$$I_z.\ddot{\psi} + (-\mathring{N}_r - f_z).\dot{\psi} + (\mathring{N}_v.U\infty + K).\psi = 0 \qquad \text{EQN(14)}$$

where $K = l^2.(k4 + k5)$

l = distance from c.g. to wire attachment point = 0.46m

$k4+k5$ = sum of spring constants = 63.5 N/m

Comparing equation (14) with the appropriate equations of the form of (5) and (6) leads to the identities:

$$a = 2\zeta\omega_{o_{on}} = -2\mu_{on} = (-\mathring{N}_r - f_z)/I_z \qquad \text{EQN(15)}$$

$$\text{and} \quad b = \omega_{o_{on}}^2 = (U\infty\mathring{N}_v + K)/I_z \qquad \text{EQN(16)}$$

WIND-OFF:

If the model is tested with the wind-off, the aerodynamic terms of (15) and (16) may be neglected since $\mathring{N}_v \cong 0$ and $\mathring{N}_r \cong 0$. Further, $U\infty$ will be zero and the following terms may be defined for the wind-off case:

$$I_z = [l^2(k_1 + k_2)]/(\omega_{o_{off}}^2) \qquad \text{EQN(17)}$$

$$f_z = 2.I_z.\mu_{off} \qquad \text{EQN(18)}$$

Experimental Wind-off Data: (from file Y10C.C8)

$T_{off} = 0.61$ (s) $\omega_n^2 = 106.096$ (r/s)^2

$\mu_{off} = -0.459$ (r/s) $\omega_{o\,off}^2 = 106.307$ (r/s)^2

Substituting the above values into equations (17) and (18) gives:

$I_z = 0.126$ kgm^2 or 0.093 slug.ft^2 (cf 0.096 kgm^2 expected)

$f_z = -0.184$ kgm^{2}r/s

WIND-ON:

Using (15) and noting that $f_z/I_z = 2\mu_{off}$ it can be shown that:

$$\mathring{N}_r = 2.I_z.(\mu_{on} - \mu_{off}) \qquad \text{EQN(19)}$$

Similarly, using (16) and noting that $K/I_z = \omega_{off}^2$ it may be shown that:

$$\mathring{N}_v = (I_z/U\infty).(\omega_{o\,on}^2 - \omega_{o\,off}^2) \qquad \text{EQN(20)}$$

Experimental Wind-on Data: (from file Y10ONC.C8)

$T_{on} = 0.55$ (s) $\omega_n^2 = 130.507$ (r/s)^2

$\mu_{on} = -0.893$ (r/s) $\omega_{o\,on}^2 = 131.304$ (r/s)^2

Substituting the appropriate wind-off and wind-on values into equations (19) and (20) leads to

$\mathring{N}_v = 0.099$ kg.m/s

$\mathring{N}_r = -0.109$ kg.m^2/s

The experimental data wind-on was recorded at a tunnel speed of 63.8 mm H_2O which corresponds to $U\infty$ = 32.73 m/s.

The model parameters S = 0.115 m^2 and b = 0.782 m yields the following to non-dimensionalise the derivatives:

$$N_v = \mathring{N}_v / (0.5).\rho.U\infty.S.b = \mathring{N}_v / 1.7478$$

$$N_r = \mathring{N}_r / (0.5).\rho.U\infty.S.b^2 = \mathring{N}_r / 1.3667$$

$$\Rightarrow N_v = 0.057 \quad \text{and} \quad \Rightarrow N_r = -0.08$$

Appendix B gives details of the theoretical values of these non-dimensional derivatives (estimated by Malik and from REF 7). The results are summarised below, along with the percentage relative error between these results and the values of derivatives obtained experimentally.

Table 2

	Experimental	Theoretical (%) (B.Ae.)	Estimated (%) (Malik)
N_v	0.057	0.086 (33%)	0.084 (32%)
N_r	-0.080	-0.222 (64%)	-0.103 (22%)

4.3 ROLL

The reduced model equation of motion in roll may be expressed as follows (REF 5):

$$\mathring{L}(t) = -\mathring{L}_v.v - \mathring{L}_p.p + I_x.\dot{p} - \mathring{L}_r.r \qquad \text{EQN(21)}$$

If the oscillations are assumed to be purely a rolling action of the model the yawing term ($\mathring{L}_p$) and side slip term ($\mathring{L}_v$) may be ignored. Noting that $p = \dot{\phi}$; $\dot{p} = \ddot{\phi}$; and introducing the spring stiffness term ($K.\phi$) and frictional term ($f_z.\phi$) leads to:

$$I_x.\ddot{\phi} + (-\mathring{L}_p - f_x).\dot{\phi} + (K).\phi = 0 \qquad \text{EQN(22)}$$

where $K = l^2.(k4 + k5)$

l = distance from c.g. to wire attachment point = 0.21m

$k4+k5$ = sum of spring constants = 63.5 N/m

Comparing equation (22) with the appropriate equations of the form of (5) and (6) leads to the identities:

$$a = 2\zeta\omega_{o_{on}} = -2\mu_{on} = (-\mathring{L}_p - f_x)/I_x \qquad \text{EQN(23)}$$

$$\text{and} \quad b = \omega_{o_{on}}^2 = (K)/I_z \qquad \text{EQN(24)}$$

WIND-OFF:

As the model is tested with the wind-off, the aerodynamic term $\mathring{L}_p$ of equation (23) is assumed negligible leading to the equations:

$$I_x = [l^2(k_1 + k_2)]/(\omega_{o_{off}}^2) \qquad \text{EQN(25)}$$

$$f_x = 2.I_x.\mu_{off} \qquad \text{EQN(26)}$$

Experimental Wind-off Data: (from file R24B.C8)

$T_{off} = 0.65$ (s) $\omega_n^2 = 93.440$ (r/s)^2

$\mu_{off} = -0.094$ (r/s) $\omega_{o\,off}^2 = 93.449$ (r/s)^2

Substituting the above values into equations (25) and (26) gives:

$I_x = 0.030$ kgm^2 or 0.022 slug.ft^2 (cf 0.022 kgm^2 expected)

$f_x = -0.006$ kgm^{2}r/s

5.0 MSR PROGRAM.

It was decided to try to test the MSR FORTRAN 77 program using data obtained from the inertia experiments. For example, the yaw oscillation equation: $\ddot{\psi} + a.\dot{\psi} + b.\psi = 0$

may be re-written as $\ddot{\psi} = -a.\dot{\psi} - b.\psi$

which is of the form $y = \beta_o + \beta_1.x_1 + \beta_2.x_2$

The various attitude angles were differentiated twice to produce the data required for the MSR program using the TURBO-BASIC program CONDIF.BAS.

Unfortunately it was not possible to get any sensible results from the data for oscillations in pitch, yaw or roll. Initially, this was thought to be due too few data points being used for the MSR proceedure. However, it was discovered later that the equation for the second differential y" had been wrongly programmed in the CONDIF BASIC program. This has now been corrected.

6.0 CONCLUSION.

The initial experimentation with the dynamic rig has enabled the data acquisition system to be tested and improved. Various computer routines for the smoothing of data and the subsequent formatting of recorded data are in place. Geometrical definitions of $\bar{c}$ have been sorted out and measured on the model and control surface angle calibrations have been completed. Finally, the moments of inertia of the model have been estimated, along with various aerodynamic damping derivatives.

The following list of objectives is planned for the next quarter:

1. To calibrate the pitch, roll and yaw attitude angles.

2. Integrators and summers on the ECU will be used to derive attitude rate data for recording and use in control feedback loops. Other methods of differentiating analogue data will be investigated and numerical methods will be developed further.

3. Experimentation with the pulse/doublet generator will be carried out to see what duration and magnitudes of these inputs best excite the model.

4. Recording of response data for various control surface inputs and control loops will be performed.

REFERENCES.

1. MOD AGREEMENT No.2082/192: Use of a Stepwise Regression Method with Dynamic Rig Data. October 1988.

2. HINDS. H.A. and COOK. M.V.: Measurement of the Longitudinal Static Stablity and the Moments of Inertia of a 1/12th Scale Model of a B.Ae. Hawk. College of Aeronautics Report No. P9009, Cranfield Inst. Of Technology, May 1990.

3. CAMBRIDGE ELECTRONIC DESIGN LTD.: SPECTRUM Array Arithmetic Library for MSDOS. December 1987.

4. HOROWITZ P. and HILL W.: The Art of Electronics. Cambridge University Press, 1980.

5. HINDS H.A. and COOK M.V.: Preliminary Studies for Aircraft Parameter Estimation Using Modified Stepwise Regression. College of Aeronautics Report No. p8911, Cranfield Inst. of Technology, November 1989.

6. MALIK I.A.: The Design, Development and Evaluation of an Active Control Aircraft Model Wind Tunnel Facility. 1982 College of Aeronautics Ph.D Thesis, Cranfield Inst. of Technology.

7. HAWKER SIDDELEY AVIATION LTD.: Aerodynamic Data and Stability and Derivatives of the Hawker Sideley H.S. 1182. Airframe Engineering Note AERO 1880. July 1971.

8. BABISTER A.W.: Aircraft Dynamic Stability and Response. !st Edition, Pergamon Press, 1980.

APPENDIX A

GRAPHICAL ANALYSIS OF DATA

APPENDIX A: GRAPHICAL ANALYSIS OF DATA.

The following analysis applies to the estimation of various terms for both wind-on and wind-off conditions.

To obtain T, the damped period of the oscillatory motion:

The damped oscillations of the Hawk model are recorded as output voltages produced on the electronic control unit, using the CED1401 data acquisition system. The data files stored on the IBM PC are then filtered to remove high frequency noise and centered around 0 Volts. From the smoothed data files the values of the peaks and troughs and the times at which these occur are noted. This enables the average value of the damped period (T) of the motion to be found; (eg. the average time from peak to peak).

To obtain ω_n, the system damped natural frequency:

This obtained simply from the damped period of oscillation using the formula:

$$\omega_n = \frac{2\pi}{T} \qquad \text{EQN(A1)}$$

To obtain μ, a damping factor = $-\zeta\omega_o$:

A general solution to the oscillatory motion may be expressed as:

$$\theta = A \, .e^{-\mu t}.\cos(\omega_n t + \delta) \qquad \text{EQN(A2)}$$

where:

δ is some initial angle of the recorded oscillations at t = 0.

When $\cos(\omega_n t + \delta) = 1$, this corresponds to the maximum and minimum peaks of the recorded oscillations. Thus taking two arbitrary maximum peaks, A_0 and A_1 at times t_0 and t_1, it is possible to show:

$$\ln\left(\frac{A_0}{A_1}\right) = \mu.(t_1 - t_0) = \mu.T$$

Further: $$\ln\left(\frac{A_0}{A_2}\right) = \mu.(t_2 - t_0) = \mu.2T$$

$$\ln\left(\frac{A_0}{A_3}\right) = \mu.(t_3 - t_0) = \mu.3T \quad \ldots \quad \text{etc.}$$

Thus a graph of $\ln(A_0/A_n)$ against n will produce a straight line graph of gradient μT.

μ may then be calculated from the gradient divided by the damped period T.

To obtain ω_o, the undamped natural frequency of oscillation:

The damped and undamped natural frequencies of oscillation are related by the well known relationship:

$$\omega_n = \omega_o.(1-\zeta^2)^{1/2} = \frac{2\pi}{T} \qquad \text{EQN(A3)}$$

Using the relationship $\zeta^2 = (\mu)^2/(\omega_o^2)$ and substituting this into (A3) gives:

$$\omega_o^2.\left[\ 1 - \frac{\mu^2}{\omega_o^2}\ \right] = \frac{4\pi^2}{T^2} = \omega_n^2$$

and hence $\Rightarrow$ $$\omega_o^2 = \omega_n^2 + \mu^2 \qquad \text{EQN(A4)}$$

APPENDIX B

ESTIMATION OF NON-DIMENSIONAL DERIVATIVES

APPENDIX B: ESTIMATION OF NON-DIMENSIONAL DERIVATIVES.

B.1 LONGITUDINAL DERIVATIVES.

The correct position for the aerodynamic mean chord $\bar{\bar{c}}$ has now been measured on the Hawk model. The leading edge of $\bar{\bar{c}}$ is estimated to lie 45mm behind the original reference line which was originally chosen for convenience during the longitudinal static stability experiments (REF 2). This means that the positions of the neutral point and gimbal/c.g. estimated from REF 2 should be properly expressed as $h_n = 0.412\bar{\bar{c}}$ and $h = 0.314\bar{\bar{c}}$.

The nondimensional derivative M_w may be estimated from the following formula, (REF 8), where $K_n = h_n - h$:

$$M_w = -(dC_L/d\alpha).\ K_n$$

Malik, (REF 6) estimated $h_n = 0.365\bar{\bar{c}}$ and $dC_L/d\alpha = 4.93 rad^{-1}$ from various ESDU sheets and data on the full scale Hawk. Using these figures and noting the model c.g. to be at $h = 0.314\bar{\bar{c}}$ leads to the theoretical value of $M_w = -0.248$.

However, using the longitudinal static stability data where $h_n = 0.412\bar{\bar{c}}$ and $dC_L/d\alpha = 3.7 rad^{-1}$ leads to an estimated value of $M_w = -0.363\bar{\bar{c}}$.

B.2 LATERAL DERIVATIVES.

From information of the full scale B.Ae. Hawk (REF 7) the theoretical values of $N_v = 0.086$ and $N_r = -0.222$ were estimated for $h = 0.275\bar{\bar{c}}$.

Malik (REF 6) gave the following estimates for $N_v = 0.084$ and $N_r = -0.103$.